



Published in final edited form as:

Neurosci Res. 2022 November ; 184: 9–18. doi:10.1016/j.neures.2022.07.003.

Bicuculline Restores Frequency-Dependent Hippocampal I/E Ratio and Circuit Function in PGC-1 α Null Mice

Dwipayan Bhattacharya, Ph.D.^{1,*}, Aundrea F. Bartley, Ph.D.¹, Qin Li, Ph.D.¹, Lynn E. Dobrunz, Ph.D.¹

¹Department of Neurobiology, Civitan International Research Center, and Evelyn F. McKnight Brain Institute, University of Alabama at Birmingham, 1825 University Blvd., Birmingham, AL

Abstract

Altered inhibition/excitation (I/E) balance contributes to various brain disorders. Dysfunctional GABAergic interneurons enhance or reduce inhibition, resulting in I/E imbalances. Differences in short-term plasticity between excitation and inhibition cause frequency-dependence of the I/E ratio, which can be altered by GABAergic dysfunction. However, it is unknown whether I/E imbalances can be rescued pharmacologically using a single dose when the imbalance magnitude is frequency-dependent. Loss of PGC-1 α (peroxisome proliferator activated receptor γ coactivator 1 α) causes transcriptional dysregulation in hippocampal GABAergic interneurons. PGC-1 α ^{-/-} slices have enhanced baseline inhibition onto CA1 pyramidal cells, causing increased I/E ratio and impaired circuit function. High frequency stimulation reduces the I/E ratio and recovers circuit function in PGC-1 α ^{-/-} slices. Here we tested if using a low dose of bicuculline that can restore baseline I/E ratio can also rescue the frequency-dependent I/E imbalances in these mice. Remarkably, bicuculline did not reduce the I/E ratio below that of wild type during high frequency stimulation. Interestingly, bicuculline enhanced the paired-pulse ratio (PPR) of disynaptic inhibition without changing the monosynaptic inhibition PPR, suggesting that bicuculline modifies interneuron recruitment and not GABA release. Bicuculline improved CA1 output in PGC-1 α ^{-/-} slices, enhancing EPSP-spike coupling to wild type levels at high and low frequencies. Our results show that it is possible to rescue frequency-dependent I/E imbalances in an animal model of transcriptional dysregulation with a single treatment.

Keywords

Bicuculline; E/I ratio; Feedforward Inhibition; Interneuron; E-S coupling; Short-term plasticity

1. Introduction

The balance between inhibitory and excitatory synaptic transmission (I/E balance) is responsible for shaping the dynamic homeostatic plasticity required for physiological information processing in the brain (Turrigiano and Nelson, 2004). The I/E balance helps to

*Current Address: Dwipayan Bhattacharya, Lake Erie College of Osteopathic Medicine, 1858 W. Grandview Blvd., Erie, PA 16509.
Corresponding Author: Lynn E. Dobrunz, University of Alabama at Birmingham, 1825 University Blvd, SHEL 902, Birmingham, AL 35294, dobrunz@uab.edu.

maintain neuronal firing patterns within tightly controlled ranges to establish stable circuit output in different brain regions (Bhatia et al., 2019; Murphy and Miller, 2009; Tatti et al., 2017), and is essential for efficient neural coding (Zhou and Yu, 2018). The ratio of I/E varies widely among neuronal subtypes as well as during developmental stages (Gulyás et al., 1999; Liu, 2004; Zhang et al., 2011). As a result, alterations in the I/E balance can disrupt the maturation of neuronal circuits, leading to behavioral impairments (Kehrer et al., 2008; Lee et al., 2017; Lewis et al., 2003; Nelson and Valakh, 2015). Evidence suggests that neuropsychiatric and neurological disorders share imbalances in I/E ratio as a common phenomenon (Bi et al., 2020; Canitano and Pallagrosi, 2017; Gao and Penzes, 2015). I/E balance is thought to be reduced in some disorders such as schizophrenia, autism, and Alzheimer's Disease (Bernardino et al., 2022; Canitano and Pallagrosi, 2017; Lee et al., 2017; Oliveira et al., 2018; Rubenstein and Merzenich, 2003), but enhanced in others, including Down Syndrome (Kleschevnikov et al., 2004). Similarly, disruption of the I/E balance by pharmacological perturbations of either glutamatergic excitation or GABAergic inhibition causes circuit dysfunction and behavioral deficits (Auger and Floresco, 2014; Krystal et al., 2003; Mohammadian et al., 2022; Yizhar et al., 2011). A proper understanding of the mechanisms underlying I/E imbalance is necessary to determine pharmacological targets and effective treatment strategies for multiple disorders (Gao and Penzes, 2015).

Inhibitory GABAergic transmission provides a check on the overall output of networks by preventing uncontrolled excitatory drive in neuronal circuits (Bartos and Elgueta, 2012). In addition to limiting spike generation, GABAergic interneurons play an important role in regulating spike timing and synchronization (Bartley and Dobrunz, 2015; Jang et al., 2020; Pouille and Scanziani, 2001). GABAergic neurons exert control not only of the principal neurons but also of other inhibitory neurons (Galarreta and Hestrin, 2002; Gibson et al., 1999; Pelkey et al., 2017). Therefore, changes in GABAergic inhibitory control can have complex effects on the I/E balance in neuronal circuits. For example, reduced GAD67 expression is observed in parvalbumin positive interneurons in the dorsolateral prefrontal cortex of adults with schizophrenia, resulting in impairment of inhibitory control of pyramidal cells and gamma oscillations (Lewis et al., 2012). Impaired excitatory drive onto interneurons may also cause disruption of neuronal synchrony in brain circuitry (Choi et al., 2018; Hashimoto et al., 2003; Marín, 2012). Because I/E imbalance in disease is often caused by changes in GABAergic inhibition (Kramvis et al., 2020; Nomura, 2021; Selten et al., 2018), it is important to understand if impaired I/E ratio can be restored back to optimal condition by pharmacological modulation of inhibition.

The I/E balance can be dynamic, as a result of frequency-dependent changes mediated by synaptic short-term plasticity (Bartley and Dobrunz 2015; Grangeray-Vilmint et al. 2018). There are differences in the short-term plasticity of excitatory and inhibitory synapses onto excitatory neurons (Bartley and Dobrunz, 2015), with excitatory synapses in hippocampus typically showing short-term facilitation (Dobrunz and Stevens, 1997; Zucker and Regehr, 2002) whereas inhibitory synapses usually have short-term depression (Maccaferri et al., 2000; Szabó et al., 2010). In addition, short-term plasticity differs between excitatory inputs onto excitatory and inhibitory cells (Blackman et al., 2013; Pelkey and McBain, 2007; Sun et al., 2018, 2005; Wierenga and Wadman, 2003), and between different subtypes of inhibitory cells (Beierlein et al., 2003; Li et al., 2017; Losonczy et al., 2002; Ma et al.,

2012; Sun and Dobrunz, 2006). Facilitation of excitatory inputs onto interneurons can cause frequency-dependent increases in interneuron recruitment, leading to short-term facilitation of feedforward inhibition (Bartley and Dobrunz, 2015; Nanou et al., 2018). Short-term plasticity of inhibitory inputs onto interneurons may also influence their recruitment (Patenaude et al., 2005). In hippocampus, the net result is paired-pulse depression of the I/E ratio onto CA1 pyramidal cells in response to stimulation of Schaffer collateral axons (Bartley and Dobrunz, 2015; Bartley et al., 2015; Nanou et al., 2018). The effect of reducing inhibition on the dynamics of the I/E ratio in CA1 pyramidal cells is not yet known.

Fast spiking GABAergic interneurons containing the Ca²⁺-binding protein parvalbumin have a powerful role in regulating the output of excitatory pyramidal neurons and influencing behavior (Cardin, 2018; Selten et al., 2018). Functional deficiency of parvalbumin+ interneurons is prominently observed in diseases such as schizophrenia and autism, resulting in alterations in I/E balance and circuit function (Ferguson and Gao, 2018). The transcriptional coactivator peroxisome proliferator-activated receptor γ coactivator 1 α (PGC-1 α) is required for the expression of parvalbumin and other synaptic proteins essential for neurotransmitter release (Lucas et al., 2014, 2010). Studies from postmortem schizophrenia brain have shown reduced expression of parvalbumin and complexin I (Eyles et al., 2002; Knable et al., 2004; Sawada et al., 2005), which are also observed in mice lacking PGC-1 α (Lucas et al., 2014). Other PGC-1 α dependent gene transcripts are also reduced in post mortem schizophrenia, suggesting that there is a disruption of a PGC-1 α -dependent transcriptional program in the disease (McMeekin et al., 2016). PGC-1 α mice therefore provide a model for studying the effects of interneuron transcriptional dysregulation on I/E balance and circuit function.

Our lab has previously shown that PGC-1 α null mice have enhanced GABAergic feedforward inhibition in response to stimulation of the Schaffer collateral pathway, which greatly increases the I/E ratio onto CA1 pyramidal cells (Bartley et al., 2015; Brady et al., 2016). Loss of PGC-1 α also changes the dynamics of feedforward inhibition; as a result, the extent of I/E imbalance in PGC-1 α null slices is reduced at short paired-pulse intervals (Bartley et al., 2015). This shows that the effect of interneuron transcriptional dysregulation on the I/E balance is frequency-dependent and suggests possible frequency-dependent alterations in the recruitment of feedforward interneurons. Because the extent of I/E imbalance in PGC-1 α ^{-/-} slices varies depending upon the stimulus pattern, it is uncertain whether it can be pharmacologically restored by reducing inhibition.

Here we tested the extent to which reducing inhibition can restore the dynamic I/E balance and rescue the deficits in circuit function in PGC-1 α null slices. We tested the effect in PGC-1 α ^{-/-} slices of a low dose of bicuculline methiodide (Bic, 1 μ M), which partially blocks GABA_A receptors and small-conductance calcium-activated potassium channels (SK channels) (Khawaled et al., 1999; Nowak et al., 1982). Surprisingly, we find that Bic rescues the I/E balance in PGC-1 α ^{-/-} slices during paired-pulse stimulation as well as at baseline. Bic increases the paired-pulse ratio (PPR) of disynaptic inhibition in PGC-1 α null slices, suggesting that it is altering interneuron recruitment. Bic also improves CA1 output in slices from PGC-1 α null mice to levels comparable to wild type, as measured by EPSP-Spike

(E-S) coupling. Our results show that pharmacology can potentially rescue I/E imbalances even when they are frequency-dependent.

2. Materials and Methods

2.1 Animals:

University of Alabama at Birmingham Institutional Animal Care and Use Committee approved all animal experiments performed. All experiments were conducted in accordance with the *Guide for the Care and Use of Laboratory Animals* adopted by the National Institutes of Health. Global (germline) PGC-1 α ^{-/-} mice (Lin et al., 2004) were maintained on a C57BL/6J genetic background and housed in a 26 ± 2°C room with food and water *ad libitum*. All experiments were conducted using 5- to 9-week-old male and female global PGC-1 α line (PGC-1 α ^{+/+} and PGC-1 α ^{-/-} littermates) generated by breeding PGC-1 α ^{+/-} mice (JAX # 008597; (Lin et al., 2004). Mouse genotypes were determined from tail biopsies using real time PCR with specific probes designed for PGC-1 α (Transnetyx, Cordova, TN).

2.2 Slice preparation:

Mice were anesthetized with isoflurane, decapitated, and brains rapidly removed. Then, 400- μ m-thick coronal slices of hippocampus were prepared using a vibrating microtome (Ci 7000 SMZ2; Camden) using standard methods (Sun and Dobrunz, 2006; Sun et al., 2009, 2005). Slicing and dissection of the hippocampi were done in ice-cold (1–3°C) dissecting solution containing the following (in mM): 120 NaCl, 3.5 KCl, 0.75 CaCl₂, 4.0 MgCl₂, 1.25 NaH₂PO₄, 26 NaHCO₃, and 10 glucose, bubbled with 95% O₂/5% CO₂, pH 7.35–7.45. Slices were incubated in a holding chamber containing the dissecting solution at room temperature continuously bubbled with 95% O₂–5% CO₂ for 1 h before recording.

2.3 Electrophysiology:

Electrophysiology experiments were performed in a submersion recording chamber perfused (2.5–3.5 mls/min) with external recording solution (ERS) at temperatures between 28°C and 30°C. ERS contained the following compounds (in mM): 120 NaCl, 3.5 KCl, 2.5 CaCl₂, 1.3 MgCl₂, 1.25 NaH₂PO₄, 26 NaHCO₃, and 10 glucose, bubbled with 95% O₂/5% CO₂, pH 7.35–7.45. For whole cell recordings, the ERS contained 50 μ M D-APV (D-2-amino-5-phosphonopentanoic acid) to block NMDA receptor-mediated currents; 1 μ M AM251 (N-(piperidin-1-yl)-5-(4-iodophenyl)-1-(2,4-dichlorophenyl)-4-methyl-1H-pyrazole-3-carboxamide) to block CB1 receptors and prevent depolarization-induced suppression of inhibition (De-May and Ali, 2013); and 10 μ M CGP 55845 ((2S)-3-[[[(1S)-1-(3,4-Dichlorophenyl)ethyl]amino-2-hydroxypropyl] (phenylmethyl)phosphinic acid) to block GABA_B receptors, including the receptors localized presynaptically at Schaffer collateral synapses, thereby preventing activity-dependent reduction in glutamate release (Speed and Dobrunz, 2008). To isolate monosynaptic inhibitory postsynaptic currents (IPSCs), 10 μ M NBQX (2,3-dioxo-6-nitro-1,2,3,4-tetrahydrobenzo[f]quinoxaline-7-sulfonamide) was added to the ERS. For the EPSP-spike coupling experiments no antagonists were added to the ERS. For the PGC-1 α ^{-/-} and bicuculline condition, a sub-maximal dose (1 μ M) of bicuculline methiodide (Bic)

was used to reduce the strength of GABAergic inhibition in PGC-1 α ^{-/-} slices to the level observed in PGC-1 α ^{+/+} slices.

2.4 Pyramidal whole-cell recording:

CA1 pyramidal cells were blindly patched on a Zeiss Axioskop microscope and recorded in the voltage-clamp configuration using an Axoclamp 200B amplifier (Molecular Devices). Patch electrodes (4–6M Ω) were filled with internal solution composed of the following (in mM): 125 Cs-gluconate, 0.6 EGTA, 1.0 MgCl₂, 3 MgSO₄, 25 HEPES, 10 Na-ATP, 0.3 GTP, 5 phosphocreatine, pH was adjusted to 7.2 with CsOH. The internal solution also contained 10 mM Cs-BAPTA to block depolarization induced suppression of inhibition (Isokawa and Alger, 2005) and QX-314 (*N*-(2,6-dimethylphenyl)carbamoylmethyl) triethylammonium chloride) (2 mM) to improve space clamp and to reduce nonlinear effects caused by voltage-gated channels in dendrites while recording from the soma (Colling and Wheal, 1994). The access resistance and holding current (<250 pA) were monitored continuously. Recordings were rejected if either access resistance or holding current increased >30% during the experiment.

Synaptic responses were measured in response to extracellular stimulation by a bipolar tungsten microelectrode (FHC). Stimulation was applied with a BSI-2 biphasic stimulus isolator (BAK Electronics). The stimulation intensity ranged from 10 to 200 μ A unless otherwise noted and the duration of stimulation was 100 μ s. Except where noted, the stimulating electrode was placed in stratum radiatum to stimulate the Schaffer collateral axons and positioned between 250 and 400 μ m away from the cell being recorded. Paired-pulse stimulation at different intervals (in ms: 60 and 1000) were applied and repeated 15–20 times for each interval at 0.07 Hz. Paired-pulse ratios are calculated as the amplitude of response 2/amplitude of response 1.

Disynaptic IPSCs were recorded at 0 mV (reversal potential for excitation) in the absence of NBQX. Excitatory postsynaptic currents (EPSCs) were recorded at –60 mV (reversal potential for inhibition). To record disynaptic IPSCs and EPSCs, the stimulating electrode was placed in stratum radiatum. In most cases, the disynaptic IPSCs and EPSCs were recorded from the same cell to measure the I/E ratio. Previously it was demonstrated that excitation was not altered in the PGC-1 α ^{-/-} slices (Bartley et al., 2015). Therefore, the stimulation intensity was based on the size of the EPSC generated. The stimulation intensity was set to obtain an EPSC amplitude between 90 and 250 pA. The same stimulus intensity was used to record the disynaptic IPSCs. The I/E ratio was calculated as the peak IPSC amplitude/peak EPSC amplitude.

To record monosynaptic IPSCs, the stimulating electrode was placed in or near stratum pyramidale to specifically stimulate somatic inhibition. The CA1 pyramidal cell was held at 0 mV to generate an outward inhibitory response. The maximal IPSC amplitude was determined and the stimulation was reduced to generate a response with an amplitude 30–40% of the maximum IPSC.

2.5 EPSP-spike (E-S) coupling recording:

Two field recording electrodes were used, one in stratum pyramidale to measure the population spike and the other in stratum radiatum to measure the dendritic field postsynaptic potential (fPSP) in the slice. Stimulation was applied every 10 s as a pair of pulses 60 ms apart or 1000 ms apart. A stable baseline was obtained before applying a pseudorandom series of stimulus intensities (20–450 μ A). For each experiment, the stimulus intensity was set to give fPSP amplitudes in a specific range (0.1 mV to 2.5 mV). For analysis, the initial slope of the fPSP was measured, which corresponds to the excitatory postsynaptic potential of the fPSP. The population spike amplitude was calculated by measuring the amplitude of the negative peak and adding it to the average response size of the two positive peaks, as described previously (Bartley et al., 2015; Marder and Buonomano, 2003). The data were fitted using a Boltzmann curve. Experiments were excluded if the Boltzmann curve failed to fit or if a plateau of spiking was not observed.

2.6 Statistics:

Statistics were calculated using Origin software, with statistical significance of $p < 0.05$. Data are presented as mean \pm standard error of the mean (SE) and sample number (n) refers to cell number in whole cell recordings. In EPSP-spike coupling sample number (n) refers to the number of slices. Statistical comparisons were made using one-way ANOVA or two-way ANOVA followed by Bonferroni post hoc analysis, or using paired t-test between two groups for monosynaptic IPSCs. NS = not significant; * = $p < 0.05$.

3. Results

3.1 Reducing inhibition with Bic improved the I/E ratio in PGC-1 α ^{-/-} slices

We have previously shown that loss of PGC-1 α increases the I/E ratio onto CA1 pyramidal cells through enhanced feedforward (disynaptic) inhibition, with no change in excitation (Bartley et al., 2015). To investigate whether the effects caused by loss of PGC-1 α can be restored by reducing the level of inhibition, we compared disynaptic inhibition and I/E balance with and without 1 μ M bicuculline (Bic) in PGC-1 α ^{-/-} slices (knockout) and compared the two groups to PGC-1 α ^{+/+} slices (wild type). We recorded both feedforward disynaptic IPSCs (at 0 mV, the reversal potential for excitation) and EPSCs (at -60 mV, the reversal potential for inhibition) from CA1 pyramidal cells in response to Schaffer collateral (SC) stimulation. There was almost a two-fold increase in the amplitude of disynaptic IPSCs from PGC-1 α ^{-/-} slices as compared to PGC-1 α ^{+/+} (Figure 1A), consistent with our previous results (Bartley et al., 2015). Bic significantly reduced the disynaptic IPSC amplitude in PGC-1 α ^{-/-} slices (Figure 1A), to a level that was no longer significantly different from PGC-1 α ^{+/+} slices (Figure 1A). There was no statistical significant difference in the EPSC amplitude among the three groups PGC-1 α ^{-/-}, BicPGC-1 α ^{-/-} and PGC-1 α ^{+/+} (Figure 1B), indicating that Bic had no effect on the EPSC amplitude in PGC-1 α ^{-/-} slices. There was also no difference in the stimulus intensity for the three conditions (one-way ANOVA ($F_{(2,25)}=1.834$, $p=0.16$; PGC-1 α ^{+/+} $30 \pm 9.6 \mu$ A, BicPGC-1 α ^{-/-} $19.9 \pm 2.9 \mu$ A, PGC-1 α ^{-/-} $17.9 \pm 1.7 \mu$ A). The I/E ratio was therefore nearly twice as large in PGC-1 α ^{-/-} slices compared to PGC-1 α ^{+/+} (Figure 1C). Bic reduced the I/E ratio significantly in PGC-1 α ^{-/-} slices and brought it back to the level observed in PGC-1 α ^{+/+} slices (Figure 1C). Together,

these data show that reducing disynaptic IPSCs with Bic rescues the baseline I/E ratio in slices from PGC-1 $\alpha^{-/-}$ mice.

3.2 Bic improved the CA1 circuit output in PGC-1 $\alpha^{-/-}$ slices

We have previously shown that enhanced inhibition in PGC-1 $\alpha^{-/-}$ slices affects the CA1 circuit output, causing a large decrease in basal CA1 pyramidal cell spiking and reduced EPSP-Spike (E-S) coupling (Bartley et al., 2015). Here, we tested whether restoring the baseline I/E ratio with Bic can rescue the reduced CA1 output in PGC-1 $\alpha^{-/-}$ slices. We measured the initial slope of fPSP responses in stratum radiatum and population spike amplitudes in stratum pyramidale in response to SC pathway stimulation (Figure 2A). PGC-1 $\alpha^{-/-}$ slices showed consistently reduced CA1 pyramidal neuron spiking across a range of fPSP sizes in response to increasing stimulus intensities (Figure 2B), as previously reported (Bartley et al., 2015). Indeed, bath applied Bic improved the E-S coupling in CA1 pyramidal neurons in PGC-1 $\alpha^{-/-}$ slices across increasing fPSP responses. Thus, the CA1 output is no longer suppressed in PGC-1 $\alpha^{-/-}$ slices with Bic as compared to PGC-1 $\alpha^{+/+}$ slices (Figure 2B). The maximum population spike amplitude is also rescued by Bic in PGC-1 $\alpha^{-/-}$ slices and is no longer different when compared to PGC-1 $\alpha^{+/+}$ slices (Figure 2C). Together, these data show that reduced inhibition improves basal CA1 network output in PGC-1 $\alpha^{-/-}$ slices.

3.3 Frequency dependent enhancement in the I/E ratio is restored with Bic in PGC-1 $\alpha^{-/-}$ slices

Our lab has previously reported that the enhanced I/E ratio in CA1 pyramidal cells in slices from PGC-1 $\alpha^{-/-}$ mice is frequency-dependent. Specifically, the I/E ratio is largest for basal synaptic transmission (0.07 Hz), but is reduced considerably with high frequency stimulation (second pulse of paired-pulse stimulation at short paired-pulse intervals), and intermediate in magnitude at low-middle frequency stimulation (second pulse at longer paired-pulse interval) (Bartley et al., 2015). Here we also observed that the I/E ratio in PGC-1 $\alpha^{-/-}$ slices is reduced on the second pulse at the 60 ms paired-pulse interval compared to its basal (pulse 1) I/E ratio (Figure 3A vs Figure 1C) (one-way ANOVA ($F_{(2,36)} = 5.09$, $p = 0.011$), and not significantly different from that of the second pulse in PGC-1 $\alpha^{+/+}$ slices (Figure 3A). In contrast, the I/E ratio on the second pulse at 1000 ms paired-pulse interval is significantly larger in PGC-1 $\alpha^{-/-}$ slices than PGC-1 $\alpha^{+/+}$ slices (Figure 3A), although the difference is not as large as during basal transmission (Figure 1A), consistent with previous results (Bartley et al., 2015). Because the magnitude of the increase I/E ratio is variable, it is not known if a single dose of Bic can restore the I/E ratio in PGC-1 $\alpha^{-/-}$ slices on the second pulse of paired-pulse stimulation as it does for the basal I/E ratio. Here we tested the effects of 1 μ M Bic on two intervals of paired-pulse stimulation (60 ms and 1000 ms). We expected that application of Bic would reduce the I/E ratio on the second pulse at both intervals in PGC-1 $\alpha^{-/-}$ slices, based on the fact that it causes a two-fold decrease in disynaptic IPSC amplitude for pulse 1. Interestingly, there was no significant difference in the I/E ratio on the second pulse at 60 ms in PGC-1 $\alpha^{-/-}$ slices with Bic compared to PGC-1 $\alpha^{+/+}$ slices (Figure 3A), indicating that Bic did not cause the I/E ratio to be reduced past wild type levels (smaller response as compared to wild type). On the second pulse at the 1000 ms paired-pulse interval, bath applied Bic reduced the I/E ratio in PGC-1 $\alpha^{-/-}$ slices to

wild type level (Figure 3A). Therefore, a single dose of Bic can rescue the I/E imbalance in the PGC-1 α ^{-/-} slices even though it is frequency dependent.

Since Bic was able to restore the I/E ratio on the second pulse at both intervals back to wild type levels, this suggests that Bic is differentially reducing disynaptic IPSCs on the second pulse at 60 ms, compared to its effects on the first pulse (Figure 1A) and on the second pulse at the 1000 ms paired-pulse interval. To investigate this, we examined the PPR of the EPSCs and disynaptic IPSCs used to calculate the I/E ratio. No significant difference was observed in the PPR at either interval of EPSCs onto CA1 pyramidal cells among PGC-1 α ^{+/+}, PGC-1 α ^{-/-}, and PGC-1 α ^{-/-} with Bic (Figure 3B), suggesting the effect of Bic is entirely on IPSCs, as expected. We next calculated the PPR of disynaptic IPSCs at the two intervals. At the 60 ms interval, disynaptic IPSCs have robust paired-pulse facilitation in PGC-1 α ^{+/+} slices, whereas disynaptic IPSCs in PGC-1 α ^{-/-} has very little facilitation (Figure 3C), similar to our previous results (Bartley et al., 2015). There was no difference in the PPR at the 1000 ms interval between PGC-1 α ^{+/+} slices and PGC-1 α ^{-/-} slices, in agreement with our previous report (Bartley and Dobrunz, 2015). However, Bic reduced the IPSC amplitude and potentiated the PPR in PGC-1 α ^{-/-} slices at 60 ms, restoring the PPR to the level measured in PGC-1 α ^{+/+} (Figure 3C). The effect of Bic is therefore smaller on the second pulse at 60 ms compared to the first pulse, causing an increase in the PPR. In contrast, there was no effect of Bic on the PPR at 1000 ms (Figure 3C), indicating that Bic reduced the disynaptic IPSC amplitude equally on the first and second pulses at the 1000 ms interval.

Because PPR is usually inversely related to initial release probability (Dobrunz and Stevens, 1997; Zucker and Regehr, 2002), changes in PPR often indicate presynaptic changes in the probability of neurotransmitter release. However, PPR of disynaptic inhibition is also influenced by changes in the recruitment of feedforward interneurons on the second pulse (Bartley and Dobrunz, 2015). The effect of Bic to increase the PPR at 60 ms therefore suggests that Bic may either influence GABA release or the recruitment of feedforward interneurons. To determine whether Bic application alters GABA release in the PGC-1 α ^{-/-} slices, we measured the PPR of monosynaptic IPSCs on pyramidal neurons at the 60 ms paired-pulse interval with and without Bic treatment. Bic significantly reduced the amplitude of somatic GABAergic monosynaptic IPSCs on pulse 1 by more than 2-fold in PGC-1 α ^{-/-} slices (Figure 3D). However, we found no significant change in PPR of monosynaptic IPSCs with Bic in PGC-1 α ^{-/-} slices (Figure 3D), indicating that Bic treatment is not altering the probability of GABA release in PGC-1 α ^{-/-} slices.

3.4 Bic recovered frequency dependent deficit in CA1 pyramidal neuron spiking in PGC-1 α ^{-/-} slices

The effect of PGC-1 α deletion on CA1 microcircuit output also showed frequency-dependent alterations. Figures 4A–C show E-S coupling measured on the second pulse at the 60 ms paired pulse interval. The output of PGC-1 α ^{-/-} slices is slightly impaired relative to PGC-1 α ^{+/+} slices. The E-S coupling curve is shifted to the right, indicating that PGC-1 α ^{-/-} slices required a larger synaptic input before starting to plateau (Figure 4B). The output of CA1 was nearly identical between PGC-1 α ^{+/+} slices and BicPGC-1 α ^{-/-} slices

(Figure 4B), indicating that even though there was a small trend for the I/E ratio at 60 ms with the addition of bicuculline in PGC-1 α ^{-/-} slices to be smaller than in PGC-1 α ^{+/+} slices (Figure 3A), this was not reflected in the E-S coupling experiments. There was no difference among the three groups in the maximum population spike amplitude on the second pulse at this short interval (Figure 4C). Figures 4D–4F show E-S coupling measured on the second pulse at the 1000 ms paired pulse interval. Similar to the basal condition, there is a large deficit in CA1 output in PGC-1 α ^{-/-} slices at the 1000 ms interval, which again is rescued by bicuculline (Figure 4E). The maximum population spike amplitude on the second pulse at 1000 ms was significantly reduced in PGC-1 α ^{-/-} slices as compared to PGC-1 α ^{+/+} slices, and restored by Bic (Figure 4F). Together, the results show that bicuculline treatment can rescue the frequency dependent I/E imbalance and CA1 circuit output in PGC-1 α ^{-/-} slices.

4. Discussion

The goal of this study was to investigate whether a pharmacologically reducing inhibition can rescue the frequency-dependent I/E imbalance seen in mice with deletion of PGC-1 α . We used a 1 μ M dose of Bic to reduce inhibition. The dose of Bic was sufficient to significantly reduce the I/E ratio in PGC-1 α ^{-/-} slices at baseline, restoring it to a level comparable to that in wild type slices. Surprisingly, Bic has a differential effect on the I/E ratio depending on the paired-pulse interval (60 ms and 1000 ms). In particular, Bic rescued the I/E ratio of the second pulse at 1000 ms, without causing the I/E ratio to be reduced to below wild type levels on the second pulse at the 60 ms interval. Thus the same dose of Bic normalized the I/E ratio at baseline and at both short and longer paired-pulse intervals in PGC-1 α ^{-/-} slices, despite differences in the magnitude of the I/E imbalance. In addition, Bic rescued the reduced PPR of disynaptic IPSCs at 60 ms, but had no effect at 1000 ms. This was not caused by an effect on GABA release, as Bic did not alter the PPR of monosynaptic IPSCs. Reducing the I/E ratio with Bic also improved the CA1 circuit function in PGC-1 α ^{-/-} slices at baseline and at both paired-pulse intervals tested. Together our results suggest that pharmacologically targeting inhibition can improve I/E imbalances even when they are frequency dependent.

The low dose of bicuculline methiodide caused a ~60% reduction of both monosynaptic and disynaptic IPSCs. Bicuculline and its quaternary salts such as bicuculline methiodide are competitive antagonists of GABA_A receptors (Seutin and Johnson, 1999), and 1 μ M bicuculline methiodide is expected to block about half of GABA_A receptor currents (Nowak et al., 1982; Ueno et al., 1997). Bicuculline methiodide can also inhibit SK channels, the primary mediator of the medium afterhyperpolarization (Faber and Sah, 2007). SK channels are expressed in interneurons (Deister et al., 2009; Orduz et al., 2013), and blocking SK channels can potentially increase their action potential firing. The EC₅₀ of bicuculline methiodide for SK channel ranges from 1–25 μ M (Faber and Sah, 2007), so there is likely to be only a partial block of SK in our experiments. It is possible that reduced current through SK channels in interneurons contributes to the changes in disynaptic inhibition seen with Bic. However the effect of reduced SK channel current on baseline disynaptic inhibition is expected to be minimal, and the main mediator of bicuculline's effects is likely the block of GABA_A receptors.

An important finding is that partially blocking inhibition can restore the I/E ratio and rescue circuit function in PGC-1 α ^{-/-} slices despite the frequency-dependence of the I/E imbalance. Short-term plasticity has been shown to regulate both the I/E ratio and E-S coupling (Bartley and Dobrunz, 2015; Bartley et al., 2015; Marder and Buonomano, 2003). Paired-pulse stimulation reduces the I/E ratio (enhances the E/I ratio) at short paired-pulse intervals (Bartley and Dobrunz, 2015; Bartley et al., 2015), however the effect is more dramatic in PGC-1 α ^{-/-} slices. As a result, the magnitude of the increase in I/E ratio is greatest on the first pulse and smaller at shorter intervals. Therefore, the expectation would be that the dose of Bic that rescues the I/E ratio on the first pulse would reduce inhibition so much on the second pulse that the I/E ratio would actually be smaller in PGC-1 α ^{-/-} than in wild type slices. However, that was not observed, as there was no difference in I/E ratio between BicPGC-1 α ^{-/-} as compared to PGC-1 α ^{+/+} slices on the second pulse. Bic also rescued the deficit in E-S coupling. The increase in E-S coupling at baseline in BicPGC-1 α ^{-/-} slices (compared to PGC-1 α ^{-/-} slices) is consistent with previous studies that have shown reducing or abolishing inhibition increases the spike probability by as much as 5 fold (Bartley and Dobrunz, 2015; Pouille and Scanziani, 2001; Pouille et al., 2009). There was no enhancement (compared to PGC-1 α ^{+/+} slices) in E-S coupling on the second pulse, either because the I/E ratio was similar or possibly through a ceiling effect of reduced inhibition on spiking. There is still a possibility that at a more intermediate paired-pulse interval the low dose of bicuculline would not restore the effect back to wild type levels. Together, our results support reducing inhibition as an effective therapeutic treatment for a dynamic imbalance in E/I ratio.

Increased inhibition has been observed in other mouse models of disease, including Down Syndrome (Kleschevnikov et al., 2012, 2004), autism (Tabuchi et al., 2007) and schizophrenia (Nomura et al., 2016). It is not yet known whether the I/E imbalances in these models are frequency-dependent. Repeated administration of phencyclidine, a non-competitive N-methyl-d-aspartate (NMDA) receptor antagonist causes enhanced GABA transmission and increased long-term potentiation threshold in adult mice (Nomura et al., 2016). These mice also showed schizophrenia related deficits in cognition (Nomura et al., 2016), which were alleviated by Bic administration into hippocampus (Meltzer et al., 2018). In addition, studies using picrotoxin to partially block GABA_A receptors have been successful in rescuing some deficits in Down Syndrome mice, including impairment of long-term potentiation and behavior (Fernandez et al., 2007; Martínez-Cué et al., 2014). Loss of PGC-1 α causes behavioral deficits, including impairments in nest building behavior (Bartley et al., 2015; Brady et al., 2016) and the Barnes maze (Lucas et al., 2014), which are consistent with impaired CA1 circuit function. Administration of Bic to hippocampus may therefore improve these behavioral deficits in PGC-1 α ^{-/-} mice. Although it can be challenging to find a safe therapeutic dose, reducing inhibition may be a useful strategy to treat disorders that have enhanced GABAergic inhibition (Vinkers et al., 2010).

Interestingly, Bic was able to restore the PPR of disynaptic inhibition on the second pulse at the short paired-pulse interval in PGC-1 α ^{-/-} slices. For EPSCs and monosynaptic IPSCs, the PPR is usually inversely related to the initial release probability (Dobrunz and Stevens, 1997; Regehr, 2012; Sun et al., 2005; Zucker and Regehr, 2002), and changes in PPR often are indicative of presynaptic changes in neurotransmitter release (Regehr, 2012). While

alterations in PPR are typically a result of changes in initial release probability, changes in release probability only on the second pulse of paired stimulation can also occur (Sippy et al., 2003; Speed and Dobrunz, 2009; Walters et al., 2014). Although we find here that Bic restores the PPR of disynaptic IPSCs onto CA1 pyramidal cells in PGC-1 α ^{-/-} slices, the lack of effect on the PPR of monosynaptic IPSCs indicates that Bic is not acting to modulate presynaptic GABA release probability on either the first or second pulse. This is not surprising. GABA_A receptors are not typically found on presynaptic terminals of GABAergic synapses in hippocampus (Kullmann et al., 2005). SK channels are expressed in GABAergic interneurons (Deister et al., 2009; Orduz et al., 2013), but it is unknown if they are expressed presynaptically or postsynaptically. However, in pyramidal cells SK channels are mainly expressed postsynaptically (Faber et al., 2005; Stackman et al., 2002). It is possible that the disynaptic IPSCs are recruiting synapses from different subtypes of interneurons than were recorded for monosynaptic IPSCs, which were in response to stimulation of axons near stratum pyramidale. These somatic targeting monosynaptic IPSCs were likely composed largely of parvalbumin and cholecystokinin positive basket cells, both of which have been shown to be affected by loss of PGC-1 α (Bartley et al., 2015). Loss of PGC-1 α also has been shown to affect dendritic targeting interneurons (Bartley et al., 2015). However, neither somatic or dendritic monosynaptic IPSCs have paired-pulse facilitation in wild type slices (Bartley et al., 2015), so it is unlikely that the restoration of paired-pulse facilitation in the disynaptic IPSCs in PGC-1 α ^{-/-} slices is caused by incorporation of dendritic targeting inhibitory synapses. Therefore, the restoration of disynaptic PPR in PGC-1 α ^{-/-} slices by Bic is most likely not caused by an increase in monosynaptic PPR.

Another possible mechanism for the enhancement of disynaptic PPR in PGC-1 α ^{-/-} slices by Bic is through effects on interneuron recruitment, as illustrated in the cartoons in Figure 5. Our lab has previously shown in wild type slices that differences in interneuron recruitment between pulse 1 and pulse 2 can contribute to the PPR of feedforward disynaptic IPSCs (Bartley and Dobrunz, 2015). Feedforward inhibition in response to Schaffer collateral stimulation has paired-pulse facilitation (Bartley and Dobrunz, 2015; Nanou et al., 2018), even though GABAergic synapses onto CA1 pyramidal cells have paired-pulse depression (Maccafferri et al., 2000; Szabó et al., 2010). This results from increased recruitment of feedforward interneurons on the second pulse at short intervals (Bartley and Dobrunz, 2015). EPSCs onto most subtypes of feedforward CA1 interneurons have paired-pulse facilitation (Sun and Dobrunz, 2006; Sun et al., 2005), helping to increase spike probability on the second pulse in wild type slices (Bartley and Dobrunz, 2015). Paired-pulse depression of IPSCs onto interneurons (Ma et al., 2012) may also contribute to their enhanced spiking on the second pulse. In PGC-1 α ^{-/-} slices, in contrast, feedforward (disynaptic) IPSCs have very little paired-pulse facilitation or can even express paired-pulse depression (Bartley et al., 2015), indicating impaired recruitment of interneurons on the second pulse compared to wild type. It is not yet known whether this results from reduced paired-pulse facilitation of excitatory inputs onto CA1 interneurons (Nanou et al., 2018), reduced excitability of GABAergic interneurons (Dougherty et al., 2014), or increased PPR of GABAergic input, and which subtypes of interneurons are affected. Because Bic also partially blocks GABA_A receptors on interneurons, reducing their inhibitory input, it is tempting to speculate that altered inhibitory input onto interneurons is responsible. Additionally, partially blocking

SK channels could increase the excitability of GABAergic interneurons (Orduz et al., 2013) leading to enhanced recruitment on the second pulse. It is possible that partially blocking both GABA_A receptors and SK channels are needed to rescue the frequency-dependent imbalance seen in PGC-1 α ^{-/-} slices; a similar synergistic role occurs to generate thalamocortical oscillations (Kleiman-Weiner et al., 2009). In any case, the effect of Bic to rescue the PPR of disynaptic IPSCs onto CA1 pyramidal cells PGC-1 α ^{-/-} slices is most likely through an enhancement of interneuron spiking on the second pulse.

We have previously shown that an increase in GABA release contributes to the enhanced inhibition onto CA1 pyramidal cells in PGC-1 α ^{-/-} slices (Bartley et al., 2015). CA1 pyramidal cells in PGC-1 α ^{-/-} slices had an increase in mIPSC frequency and reduced coefficient of variation of monosynaptic IPSCs, indicating enhanced GABA release probability (Bartley et al., 2015). There was no change in mIPSC amplitude in pyramidal cells, consistent with a lack of effect of PGC-1 α ^{-/-} deletion on postsynaptic GABA_A receptors (Bartley et al., 2015). PGC-1 α is a transcription cofactor required for the expression of synaptic proteins in interneurons that are associated with neurotransmitter release, including synaptotagmin 2 and complexin 1 (Bartley et al., 2015; Lucas et al., 2014). This does not explain the enhanced GABA release in CA1 of PGC-1 α ^{-/-} slices, as loss of synaptotagmin 2 or complexin 1 would be expected to instead reduce or desynchronize GABA release (Chen et al., 2017; Yang et al., 2010). Reduced parvalbumin levels are observed in PGC-1 α ^{-/-} mice (Bartley et al., 2015; Lucas et al., 2010), which would be expected to decrease presynaptic calcium buffering, potentially enhancing GABA release. Genetic deletion of parvalbumin increases the paired-pulse ratio of GABAergic synapses (monosynaptic inhibition) (Caillard et al., 2000). Consistent with this, the paired-pulse ratio of monosynaptic inhibition is greater in PGC-1 α ^{-/-} slices (Bartley et al., 2015). Bic does not alter the paired-pulse ratio of monosynaptic inhibition in PGC-1 α ^{-/-} slice, indicating that it does not affect GABA release probability. Our results here show that bicuculline is able to balance the effect of increased release of GABA on the I/E ratio, thus reducing inhibition by a different mechanism than is altered by loss of PGC-1 α .

Because GABAergic dysfunction and resulting imbalance between excitatory and inhibitory transmission occur in a wide range of neurodevelopmental and neuropsychiatric disorders (Canitano and Pallagrosi, 2017; Gao and Penzes, 2015; Lee et al., 2017; Oliveira et al., 2018; Rubenstein and Merzenich, 2003; Selten et al., 2018), pharmacological restoration of normal I/E balance has therapeutic potential for numerous disorders. Alterations in the magnitude of I/E imbalance as a function of frequency can potentially complicate this, as a constant reduction of inhibition could cause the I/E ratio to be reduced below wild type levels at some frequencies. A key finding of our study is that bicuculline does not cause a constant reduction of disynaptic inhibition but reduces it to a lesser extent on the second pulse depending on frequency (Figure 5). As a result in a rodent model of transcriptional dysregulation, a low dose of bicuculline can restore the I/E balance even though it is frequency-dependent. This appeared to be caused by frequency-dependent modulation of interneuron recruitment by bicuculline. Future studies can investigate the role of GABA_A receptors and SK channels on interneuron recruitment. Additionally, since bicuculline blocks GABA_A receptors on both excitatory and inhibitory neurons, subtype selective GABA_A receptor modulation (Rudolph and Möhler, 2014) may be useful

for altering inhibition onto excitatory neurons or interneurons selectively, or on specific subtypes of interneurons, giving more therapeutic options. While it may not be true that the I/E balance can be restored by bicuculline at multiple frequencies in other disorders, our results highlight the importance of investigating the effects of pharmacological treatments on the frequency dependence of the inhibition/excitation balance, as well as on the recruitment of interneurons.

Acknowledgements

This work was supported by National Institutes of Health grant R01MH098534 to L.E.D.

Abbreviations

PGC-1α	peroxisome proliferator activated receptor γ coactivator 1 α
I/E	Inhibition/Excitation
Bic	bicuculline
E-S coupling	EPSP-spike coupling
ERS	external recording solution
PPR	paired-pulse ratio
SC	Schaffer collateral
IPSCs	Inhibitory postsynaptic currents
EPSCs	Excitatory postsynaptic currents
fPSP	field postsynaptic potential
SK channels	small-conductance calcium-activated potassium channels

References

- Auger ML, Floresco SB, 2014. Prefrontal cortical GABA modulation of spatial reference and working memory. *Int. J. Neuropsychopharmacol* 18.
- Bartley AF, Dobrunz LE, 2015. Short-term plasticity regulates the excitation/inhibition ratio and the temporal window for spike integration in CA1 pyramidal cells. *Eur. J. Neurosci* 41, 1402–1415. [PubMed: 25903384]
- Bartley AF, Lucas EK, Brady LJ, Li Q, Hablitz JJ, Cowell RM, Dobrunz LE, 2015. Interneuron Transcriptional Dysregulation Causes Frequency-Dependent Alterations in the Balance of Inhibition and Excitation in Hippocampus. *J. Neurosci* 35, 15276–15290. [PubMed: 26586816]
- Bartos M, Elgueta C, 2012. Functional characteristics of parvalbumin- and cholecystokinin-expressing basket cells. *J. Physiol. (Lond.)* 590, 669–681. [PubMed: 22250212]
- Beierlein M, Gibson JR, Connors BW, 2003. Two dynamically distinct inhibitory networks in layer 4 of the neocortex. *J. Neurophysiol* 90, 2987–3000. [PubMed: 12815025]
- Bernardino I, Dionísio A, Violante IR, Monteiro R, Castelo-Branco M, 2022. Motor Cortex Excitation/Inhibition Imbalance in Young Adults With Autism Spectrum Disorder: A MRS-TMS Approach. *Front. Psychiatry* 13, 860448.

- Bhatia A, Moza S, Bhalla US, 2019. Precise excitation-inhibition balance controls gain and timing in the hippocampus. *Elife* 8.
- Bi D, Wen L, Wu Z, Shen Y, 2020. GABAergic dysfunction in excitatory and inhibitory (E/I) imbalance drives the pathogenesis of Alzheimer's disease. *Alzheimers Dement.* 16, 1312–1329. [PubMed: 32543726]
- Blackman AV, Abrahamsson T, Costa RP, Lalanne T, Sjöström PJ, 2013. Target-cell-specific short-term plasticity in local circuits. *Front. Synaptic Neurosci* 5, 11. [PubMed: 24367330]
- Brady LJ, Bartley AF, Li Q, McMeekin LJ, Hablitz JJ, Cowell RM, Dobrunz LE, 2016. Transcriptional dysregulation causes altered modulation of inhibition by haloperidol. *Neuropharmacology* 111, 304–313. [PubMed: 27480797]
- Caillard O, Moreno H, Schwaller B, Llano I, Celio MR, Marty A, 2000. Role of the calcium-binding protein parvalbumin in short-term synaptic plasticity. *Proc. Natl. Acad. Sci. USA* 97, 13372–13377. [PubMed: 11069288]
- Canitano R, Pallagrosi M, 2017. Autism spectrum disorders and schizophrenia spectrum disorders: excitation/inhibition imbalance and developmental trajectories. *Front. Psychiatry* 8, 69. [PubMed: 28507523]
- Cardin JA, 2018. Inhibitory interneurons regulate temporal precision and correlations in cortical circuits. *Trends Neurosci.* 41, 689–700. [PubMed: 30274604]
- Chen C, Arai I, Satterfield R, Young SM, Jonas P, 2017. Synaptotagmin 2 is the fast Ca^{2+} sensor at a central inhibitory synapse. *Cell Rep.* 18, 723–736. [PubMed: 28099850]
- Choi SJ, Mukai J, Kvajo M, Xu B, Diamantopoulou A, Pitychoutis PM, Gou B, Gogos JA, Zhang H, 2018. A Schizophrenia-Related Deletion Leads to KCNQ2-Dependent Abnormal Dopaminergic Modulation of Prefrontal Cortical Interneuron Activity. *Cereb. Cortex* 28, 2175–2191. [PubMed: 28525574]
- Colling SB, Wheal HV, 1994. Fast sodium action potentials are generated in the distal apical dendrites of rat hippocampal CA1 pyramidal cells. *Neurosci. Lett* 172, 73–96. [PubMed: 8084540]
- De-May CL, Ali AB, 2013. Cell type-specific regulation of inhibition via cannabinoid type 1 receptors in rat neocortex. *J. Neurophysiol* 109, 216–224. [PubMed: 23054605]
- Deister CA, Chan CS, Surmeier DJ, Wilson CJ, 2009. Calcium-activated SK channels influence voltage-gated ion channels to determine the precision of firing in globus pallidus neurons. *J. Neurosci* 29, 8452–8461. [PubMed: 19571136]
- Dobrunz LE, Stevens CF, 1997. Heterogeneity of release probability, facilitation, and depletion at central synapses. *Neuron* 18, 995–1008. [PubMed: 9208866]
- Dougherty SE, Bartley AF, Lucas EK, Hablitz JJ, Dobrunz LE, Cowell RM, 2014. Mice lacking the transcriptional coactivator PGC-1 α exhibit alterations in inhibitory synaptic transmission in the motor cortex. *Neuroscience* 271, 137–148. [PubMed: 24769433]
- Eyles DW, McGrath JJ, Reynolds GP, 2002. Neuronal calcium-binding proteins and schizophrenia. *Schizophr. Res* 57, 27–34. [PubMed: 12165373]
- Faber ESL, Delaney AJ, Sah P, 2005. SK channels regulate excitatory synaptic transmission and plasticity in the lateral amygdala. *Nat. Neurosci* 8, 635–641. [PubMed: 15852010]
- Faber ESL, Sah P, 2007. Functions of SK channels in central neurons. *Clin. Exp. Pharmacol. Physiol* 34, 1077–1083. [PubMed: 17714097]
- Ferguson BR, Gao W-J, 2018. PV Interneurons: Critical Regulators of E/I Balance for Prefrontal Cortex-Dependent Behavior and Psychiatric Disorders. *Front. Neural Circuits* 12, 37. [PubMed: 29867371]
- Fernandez F, Morishita W, Zuniga E, Nguyen J, Blank M, Malenka RC, Garner CC, 2007. Pharmacotherapy for cognitive impairment in a mouse model of Down syndrome. *Nat. Neurosci* 10, 411–413. [PubMed: 17322876]
- Galarreta M, Hestrin S, 2002. Electrical and chemical synapses among parvalbumin fast-spiking GABAergic interneurons in adult mouse neocortex. *Proc. Natl. Acad. Sci. USA* 99, 12438–12443. [PubMed: 12213962]
- Gao R, Penzes P, 2015. Common mechanisms of excitatory and inhibitory imbalance in schizophrenia and autism spectrum disorders. *Curr. Mol. Med* 15, 146–167. [PubMed: 25732149]

- Gibson JR, Beierlein M, Connors BW, 1999. Two networks of electrically coupled inhibitory neurons in neocortex. *Nature* 402, 75–79. [PubMed: 10573419]
- Gulyás AI, Megías M, Emri Z, Freund TF, 1999. Total number and ratio of excitatory and inhibitory synapses converging onto single interneurons of different types in the CA1 area of the rat hippocampus. *J. Neurosci* 19, 10082–10097. [PubMed: 10559416]
- Hashimoto T, Volk DW, Eggan SM, Mirnics K, Pierri JN, Sun Z, Sampson AR, Lewis DA, 2003. Gene expression deficits in a subclass of GABA neurons in the prefrontal cortex of subjects with schizophrenia. *J. Neurosci* 23, 6315–6326. [PubMed: 12867516]
- Isokawa M, Alger BE, 2005. Retrograde endocannabinoid regulation of GABAergic inhibition in the rat dentate gyrus granule cell. *J. Physiol. (Lond.)* 567, 1001–1010. [PubMed: 16037085]
- Jang HJ, Chung H, Rowland JM, Richards BA, Kohl MM, Kwag J, 2020. Distinct roles of parvalbumin and somatostatin interneurons in gating the synchronization of spike times in the neocortex. *Sci. Adv* 6, eaay5333.
- Kehrer C, Maziashvili N, Dugladze T, Gloveli T, 2008. Altered Excitatory-Inhibitory Balance in the NMDA-Hypofunction Model of Schizophrenia. *Front. Mol. Neurosci* 1, 6. [PubMed: 18946539]
- Khawaled R, Bruening-Wright A, Adelman JP, Maylie J, 1999. Bicuculline block of small-conductance calcium-activated potassium channels. *Pflugers Arch.* 438, 314–321. [PubMed: 10398861]
- Kleiman-Weiner M, Beenhakker MP, Segal WA, Huguenard JR, 2009. Synergistic roles of GABAA receptors and SK channels in regulating thalamocortical oscillations. *J. Neurophysiol* 102, 203–213. [PubMed: 19386752]
- Kleschevnikov AM, Belichenko PV, Gall J, George L, Nosheny R, Maloney MT, Salehi A, Mobley WC, 2012. Increased efficiency of the GABAA and GABAB receptor-mediated neurotransmission in the Ts65Dn mouse model of Down syndrome. *Neurobiol. Dis* 45, 683–691. [PubMed: 22062771]
- Kleschevnikov AM, Belichenko PV, Villar AJ, Epstein CJ, Malenka RC, Mobley WC, 2004. Hippocampal long-term potentiation suppressed by increased inhibition in the Ts65Dn mouse, a genetic model of Down syndrome. *J. Neurosci* 24, 8153–8160. [PubMed: 15371516]
- Knable MB, Barci BM, Webster MJ, Meador-Woodruff J, Torrey EF, 2004. Molecular abnormalities of the hippocampus in severe psychiatric illness: postmortem findings from the Stanley Neuropathology Consortium. *Mol. Psychiatry* 9, 609–620. [PubMed: 14708030]
- Kramvis I, van Westen R, Lammertse HCA, Riga D, Heistek TS, Loebel A, Spijker S, Mansvelder HD, Meredith RM, 2020. Dysregulated prefrontal cortex inhibition in prepubescent and adolescent fragile X mouse model. *Front. Mol. Neurosci* 13, 88. [PubMed: 32528248]
- Krystal JH, D'Souza DC, Mathalon D, Perry E, Belger A, Hoffman R, 2003. NMDA receptor antagonist effects, cortical glutamatergic function, and schizophrenia: toward a paradigm shift in medication development. *Psychopharmacology* 169, 215–233. [PubMed: 12955285]
- Kullmann DM, Ruiz A, Rusakov DM, Scott R, Semyanov A, Walker MC, 2005. Presynaptic, extrasynaptic and axonal GABAA receptors in the CNS: where and why? *Prog. Biophys. Mol. Biol* 87, 33–46. [PubMed: 15471589]
- Lee E, Lee J, Kim E, 2017. Excitation/inhibition imbalance in animal models of autism spectrum disorders. *Biol. Psychiatry* 81, 838–847. [PubMed: 27450033]
- Lewis DA, Curley AA, Glausier JR, Volk DW, 2012. Cortical parvalbumin interneurons and cognitive dysfunction in schizophrenia. *Trends Neurosci.* 35, 57–67. [PubMed: 22154068]
- Lewis DA, Glantz LA, Pierri JN, Sweet RA, 2003. Altered cortical glutamate neurotransmission in schizophrenia. *Ann. N. Y. Acad. Sci* 1003, 102–112. [PubMed: 14684438]
- Li Q, Bartley AF, Dobrunz LE, 2017. Endogenously Released Neuropeptide Y Suppresses Hippocampal Short-Term Facilitation and Is Impaired by Stress-Induced Anxiety. *J. Neurosci* 37, 23–37. [PubMed: 28053027]
- Lin J, Wu P-H, Tarr PT, Lindenberg KS, St-Pierre J, Zhang C-Y, Mootha VK, Jäger S, Vianna CR, Reznick RM, Cui L, Manieri M, Donovan MX, Wu Z, Cooper MP, Fan MC, Rohas LM, Zavacki AM, Cinti S, Shulman GI, Lowell BB, Krainc D, Spiegelman BM, 2004. Defects in adaptive energy metabolism with CNS-linked hyperactivity in PGC-1alpha null mice. *Cell* 119, 121–135. [PubMed: 15454086]

- Liu G, 2004. Local structural balance and functional interaction of excitatory and inhibitory synapses in hippocampal dendrites. *Nat. Neurosci* 7, 373–379. [PubMed: 15004561]
- Losonczy A, Zhang L, Shigemoto R, Somogyi P, Nusser Z, 2002. Cell type dependence and variability in the short-term plasticity of EPSCs in identified mouse hippocampal interneurons. *J. Physiol. (Lond.)* 542, 193–210. [PubMed: 12096061]
- Lucas EK, Dougherty SE, McMeekin LJ, Reid CS, Dobrunz LE, West AB, Hablitz JJ, Cowell RM, 2014. PGC-1 α provides a transcriptional framework for synchronous neurotransmitter release from parvalbumin-positive interneurons. *J. Neurosci* 34, 14375–14387. [PubMed: 25339750]
- Lucas EK, Markwardt SJ, Gupta S, Meador-Woodruff JH, Lin JD, Overstreet-Wadiche L, Cowell RM, 2010. Parvalbumin deficiency and GABAergic dysfunction in mice lacking PGC-1 α . *J. Neurosci* 30, 7227–7235. [PubMed: 20505089]
- Ma Y, Hu H, Agmon A, 2012. Short-term plasticity of unitary inhibitory-to-inhibitory synapses depends on the presynaptic interneuron subtype. *J. Neurosci* 32, 983–988. [PubMed: 22262896]
- Maccaferri G, Roberts JD, Szucs P, Cottingham CA, Somogyi P, 2000. Cell surface domain specific postsynaptic currents evoked by identified GABAergic neurones in rat hippocampus in vitro. *J. Physiol. (Lond.)* 524 Pt 1, 91–116.
- Marder CP, Buonomano DV, 2003. Differential effects of short- and long-term potentiation on cell firing in the CA1 region of the hippocampus. *J. Neurosci* 23, 112–121. [PubMed: 12514207]
- Marín O, 2012. Interneuron dysfunction in psychiatric disorders. *Nat. Rev. Neurosci* 13, 107–120. [PubMed: 22251963]
- Martínez-Cué C, Delatour B, Potier M-C, 2014. Treating enhanced GABAergic inhibition in Down syndrome: use of GABA α 5-selective inverse agonists. *Neurosci. Biobehav. Rev.* 46 Pt 2, 218–227.
- McMeekin LJ, Lucas EK, Meador-Woodruff JH, McCullumsmith RE, Hendrickson RC, Gamble KL, Cowell RM, 2016. Cortical PGC-1 α -Dependent Transcripts Are Reduced in Postmortem Tissue From Patients With Schizophrenia. *Schizophr. Bull* 42, 1009–1017. [PubMed: 26683626]
- Meltzer H, Miyauchi M, Rajagopal L, Neugebauer N, Huang M, 2018. 257. Differential Hippocampal and Prefrontal Cortical E/I Imbalances Related to GABAA Dysfunction Contribute to the Subchronic Phencyclidine-Induced Deficits in Mouse Memory, Social Interaction and Psychosis Readout. *Biol. Psychiatry* 83, S104.
- Mohammadian F, Golitabari N, Abedi A, Saadati H, Milan HS, Salari A-A, Amani M, 2022. Early life GABAA blockade alters the synaptic plasticity and cognitive functions in male and female rats. *Eur. J. Pharmacol* 925, 174992.
- Murphy BK, Miller KD, 2009. Balanced amplification: a new mechanism of selective amplification of neural activity patterns. *Neuron* 61, 635–648. [PubMed: 19249282]
- Nanou E, Lee A, Catterall WA, 2018. Control of excitation/inhibition balance in a hippocampal circuit by calcium sensor protein regulation of presynaptic calcium channels. *J. Neurosci* 38, 4430–4440. [PubMed: 29654190]
- Nelson SB, Valakh V, 2015. Excitatory/inhibitory balance and circuit homeostasis in autism spectrum disorders. *Neuron* 87, 684–698. [PubMed: 26291155]
- Nomura T, 2021. Interneuron dysfunction and inhibitory deficits in autism and fragile X syndrome. *Cells* 10.
- Nomura T, Oyamada Y, Fernandes HB, Remmers CL, Xu J, Meltzer HY, Contractor A, 2016. Subchronic phencyclidine treatment in adult mice increases GABAergic transmission and LTP threshold in the hippocampus. *Neuropharmacology* 100, 90–97. [PubMed: 25937215]
- Nowak LM, Young AB, Macdonald RL, 1982. GABA and bicuculline actions on mouse spinal cord and cortical neurons in cell culture. *Brain Res.* 244, 155–164. [PubMed: 6288177]
- Oliveira B, Mitjans M, Nitsche MA, Kuo M-F, Ehrenreich H, 2018. Excitation-inhibition dysbalance as predictor of autistic phenotypes. *J. Psychiatr. Res* 104, 96–99. [PubMed: 30015265]
- Orduz D, Bishop DP, Schwaller B, Schiffmann SN, Gall D, 2013. Parvalbumin tunes spike-timing and efferent short-term plasticity in striatal fast spiking interneurons. *J. Physiol. (Lond.)* 591, 3215–3232. [PubMed: 23551945]

- Patenaude C, Massicotte G, Lacaille J-C, 2005. Cell-type specific GABA synaptic transmission and activity-dependent plasticity in rat hippocampal stratum radiatum interneurons. *Eur. J. Neurosci* 22, 179–188. [PubMed: 16029207]
- Pelkey KA, Chittajallu R, Craig MT, Tricoire L, Wester JC, McBain CJ, 2017. Hippocampal gabaergic inhibitory interneurons. *Physiol. Rev* 97, 1619–1747. [PubMed: 28954853]
- Pelkey KA, McBain CJ, 2007. Differential regulation at functionally divergent release sites along a common axon. *Curr. Opin. Neurobiol* 17, 366–373. [PubMed: 17493799]
- Pouille F, Marin-Burgin A, Adesnik H, Atallah BV, Scanziani M, 2009. Input normalization by global feedforward inhibition expands cortical dynamic range. *Nat. Neurosci* 12, 1577–1585. [PubMed: 19881502]
- Pouille F, Scanziani M, 2001. Enforcement of temporal fidelity in pyramidal cells by somatic feed-forward inhibition. *Science* 293, 1159–1163. [PubMed: 11498596]
- Regehr WG, 2012. Short-term presynaptic plasticity. *Cold Spring Harb. Perspect. Biol* 4, a005702.
- Rubenstein JLR, Merzenich MM, 2003. Model of autism: increased ratio of excitation/inhibition in key neural systems. *Genes Brain Behav.* 2, 255–267. [PubMed: 14606691]
- Rudolph U, Möhler H, 2014. GABAA receptor subtypes: Therapeutic potential in Down syndrome, affective disorders, schizophrenia, and autism. *Annu. Rev. Pharmacol. Toxicol* 54, 483–507. [PubMed: 24160694]
- Sawada K, Barr AM, Nakamura M, Arima K, Young CE, Dwork AJ, Falkai P, Phillips AG, Honer WG, 2005. Hippocampal complexin proteins and cognitive dysfunction in schizophrenia. *Arch. Gen. Psychiatry* 62, 263–272. [PubMed: 15753239]
- Selten M, van Bokhoven H, Nadif Kasri N, 2018. Inhibitory control of the excitatory/inhibitory balance in psychiatric disorders. [version 1; peer review: 2 approved]. *F1000Res.* 7, 23. [PubMed: 29375819]
- Seutin V, Johnson SW, 1999. Recent advances in the pharmacology of quaternary salts of bicuculline. *Trends Pharmacol. Sci* 20, 268–270. [PubMed: 10390643]
- Sippy T, Cruz-Martín A, Jeromin A, Schweizer FE, 2003. Acute changes in short-term plasticity at synapses with elevated levels of neuronal calcium sensor-1. *Nat. Neurosci* 6, 1031–1038. [PubMed: 12947410]
- Speed HE, Dobrunz LE, 2008. Developmental decrease in short-term facilitation at Schaffer collateral synapses in hippocampus is mGluR1 sensitive. *J. Neurophysiol* 99, 799–813. [PubMed: 18032567]
- Speed HE, Dobrunz LE, 2009. Developmental changes in short-term facilitation are opposite at temporoammonic synapses compared to Schaffer collateral synapses onto CA1 pyramidal cells. *Hippocampus* 19, 187–204. [PubMed: 18777561]
- Stackman RW, Hammond RS, Linardatos E, Gerlach A, Maylie J, Adelman JP, Tzounopoulos T, 2002. Small conductance Ca²⁺-activated K⁺ channels modulate synaptic plasticity and memory encoding. *J. Neurosci* 22, 10163–10171. [PubMed: 12451117]
- Sun HY, Bartley AF, Dobrunz LE, 2009. Calcium-permeable presynaptic kainate receptors involved in excitatory short-term facilitation onto somatostatin interneurons during natural stimulus patterns. *J. Neurophysiol* 101, 1043–1055. [PubMed: 19073817]
- Sun HY, Dobrunz LE, 2006. Presynaptic kainate receptor activation is a novel mechanism for target cell-specific short-term facilitation at Schaffer collateral synapses. *J. Neurosci* 26, 10796–10807. [PubMed: 17050718]
- Sun HY, Li Q, Bartley AF, Dobrunz LE, 2018. Target-cell-specific Short-term Plasticity Reduces the Excitatory Drive onto CA1 Interneurons Relative to Pyramidal Cells During Physiologically-derived Spike Trains. *Neuroscience* 388, 430–447. [PubMed: 30099117]
- Sun HY, Lyons SA, Dobrunz LE, 2005. Mechanisms of target-cell specific short-term plasticity at Schaffer collateral synapses onto interneurons versus pyramidal cells in juvenile rats. *J. Physiol. (Lond.)* 568, 815–840. [PubMed: 16109728]
- Szabó GG, Holderith N, Gulyás AI, Freund TF, Hájos N, 2010. Distinct synaptic properties of perisomatic inhibitory cell types and their different modulation by cholinergic receptor activation in the CA3 region of the mouse hippocampus. *Eur. J. Neurosci* 31, 2234–2246. [PubMed: 20529124]

- Tabuchi K, Blundell J, Etherton MR, Hammer RE, Liu X, Powell CM, Südhof TC, 2007. A neuroligin-3 mutation implicated in autism increases inhibitory synaptic transmission in mice. *Science* 318, 71–76. [PubMed: 17823315]
- Tatti R, Haley MS, Swanson OK, Tselha T, Maffei A, 2017. Neurophysiology and regulation of the balance between excitation and inhibition in neocortical circuits. *Biol. Psychiatry* 81, 821–831. [PubMed: 27865453]
- Turrigiano GG, Nelson SB, 2004. Homeostatic plasticity in the developing nervous system. *Nat. Rev. Neurosci* 5, 97–107. [PubMed: 14735113]
- Ueno S, Bracamontes J, Zorumski C, Weiss DS, Steinbach JH, 1997. Bicuculline and gabazine are allosteric inhibitors of channel opening of the GABAA receptor. *J. Neurosci* 17, 625–634. [PubMed: 8987785]
- Vinkers CH, Mirza NR, Olivier B, Kahn RS, 2010. The inhibitory GABA system as a therapeutic target for cognitive symptoms in schizophrenia: investigational agents in the pipeline. *Expert Opin. Investig. Drugs* 19, 1217–1233.
- Walters BJ, Hallgren JJ, Theile CS, Ploegh HL, Wilson SM, Dobrunz LE, 2014. A catalytic independent function of the deubiquitinating enzyme USP14 regulates hippocampal synaptic short-term plasticity and vesicle number. *J. Physiol. (Lond.)* 592, 571–586. [PubMed: 24218545]
- Wierenga CJ, Wadman WJ, 2003. Excitatory inputs to CA1 interneurons show selective synaptic dynamics. *J. Neurophysiol* 90, 811–821. [PubMed: 12904494]
- Yang X, Kaeser-Woo YJ, Pang ZP, Xu W, Südhof TC, 2010. Complexin clamps asynchronous release by blocking a secondary Ca(2+) sensor via its accessory α helix. *Neuron* 68, 907–920. [PubMed: 21145004]
- Yizhar O, Fenno LE, Prigge M, Schneider F, Davidson TJ, O’Shea DJ, Sohal VS, Goshen I, Finkelstein J, Paz JT, Stehfest K, Fudim R, Ramakrishnan C, Huguenard JR, Hegemann P, Deisseroth K, 2011. Neocortical excitation/inhibition balance in information processing and social dysfunction. *Nature* 477, 171–178. [PubMed: 21796121]
- Zhang Z, Jiao YY, Sun QQ, 2011. Developmental maturation of excitation and inhibition balance in principal neurons across four layers of somatosensory cortex. *Neuroscience* 174, 10–25. [PubMed: 21115101]
- Zhou S, Yu Y, 2018. Synaptic E-I Balance Underlies Efficient Neural Coding. *Front. Neurosci* 12, 46. [PubMed: 29456491]
- Zucker RS, Regehr WG, 2002. Short-term synaptic plasticity. *Annu. Rev. Physiol* 64, 355–405. [PubMed: 11826273]

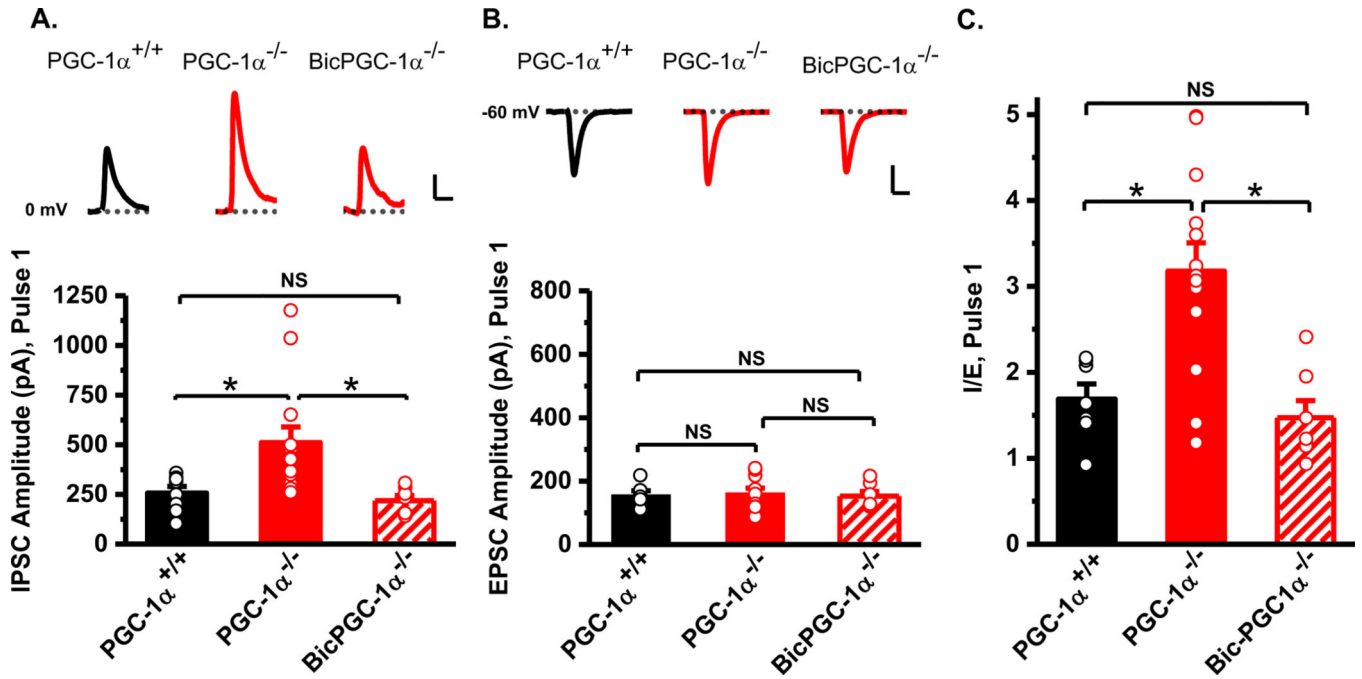


Figure 1. Bic reduces inhibition to rescue baseline I/E ratio in PGC-1 $\alpha^{-/-}$ slices.

A: The peak amplitude of disynaptic inhibition onto CA1 pyramidal cells is enhanced nearly two-fold in PGC-1 $\alpha^{-/-}$ slices compared to PGC-1 $\alpha^{+/+}$ slices. 1 μ M Bic reduced IPSC amplitude significantly in PGC-1 $\alpha^{-/-}$ slices (One-way ANOVA, $F_{(2,25)} = 5.31$, $p = 0.013$); PGC-1 $\alpha^{+/+}$ ($n = 8$), PGC-1 $\alpha^{-/-}$ ($n = 13$) and BicPGC-1 $\alpha^{-/-}$ ($n = 7$). Inset, example traces of disynaptic IPSCs from PGC-1 $\alpha^{+/+}$, PGC-1 $\alpha^{-/-}$ and BicPGC-1 $\alpha^{-/-}$ slices. Scale bars, 30 ms, 100 pA. **B:** The peak amplitude of the EPSCs is not significantly different among the three groups (One-way ANOVA, $F_{(2,25)} = 0.19$, $p = 0.83$); PGC-1 $\alpha^{+/+}$ ($n = 7$), PGC-1 $\alpha^{-/-}$ ($n = 13$) and BicPGC-1 $\alpha^{-/-}$ ($n = 7$). Inset, example traces of EPSCs from PGC-1 $\alpha^{+/+}$, PGC-1 $\alpha^{-/-}$ and BicPGC-1 $\alpha^{-/-}$ slices. Scale bars, 20 ms, 100 pA. **C:** The I/E balance in CA1 pyramidal cells, as determined from the ratio of IPSC to EPSC amplitudes, is greatly enhanced in BicPGC-1 $\alpha^{-/-}$ slices compared to PGC-1 $\alpha^{-/-}$ slices. I/E ratio in BicPGC-1 $\alpha^{-/-}$ slices do not significantly differ from PGC-1 $\alpha^{+/+}$ slices (One-way ANOVA, $F_{(2,25)} = 11.45$, $p = 0.0003$); PGC-1 $\alpha^{+/+}$ ($n = 7$), PGC-1 $\alpha^{-/-}$ ($n = 13$) and BicPGC-1 $\alpha^{-/-}$ ($n = 7$).

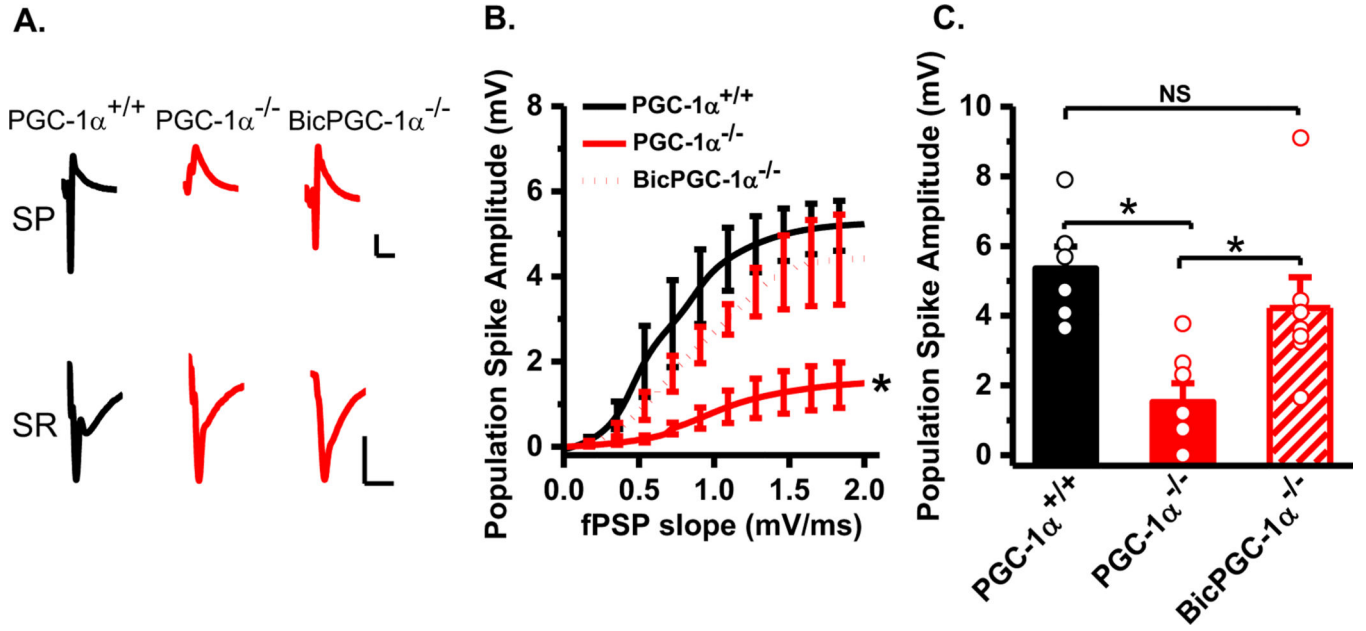


Figure 2. Bic rescues baseline CA1 circuit output in PGC-1 $\alpha^{-/-}$ slices measured with E-S coupling.

A: Example traces of field potential (fEPSP) recordings in stratum pyramidale (SP) and stratum radiatum (SR) from PGC-1 $\alpha^{+/+}$, PGC-1 $\alpha^{-/-}$, and BicPGC-1 $\alpha^{-/-}$ slices. Scale bars, 10 ms, 1mV; **B:** E-S coupling was measured from single pulse stimulation every 10 seconds. In PGC-1 $\alpha^{-/-}$ slices, the output from CA1 pyramidal cells was greatly reduced compared to PGC-1 $\alpha^{+/+}$ slices and recovered with Bic treatment (Two-way ANOVA, $F_{(2,499)} = 133.9$, $p < 0.000001$); PGC-1 $\alpha^{+/+}$ (n = 6), PGC-1 $\alpha^{-/-}$ (n = 7) and BicPGC-1 $\alpha^{-/-}$ (n = 7). * indicates significant difference from PGC-1 $\alpha^{+/+}$ and BicPGC-1 $\alpha^{-/-}$ slices. **C:** The maximum population spike generated in PGC-1 $\alpha^{-/-}$ slices was dramatically reduced compared with PGC-1 $\alpha^{+/+}$ slices. Bic treatment significantly recovered the population spike amplitude in PGC-1 $\alpha^{-/-}$ slices (One-way ANOVA, $F_{(2,17)} = 7.69$, $p = 0.0042$); PGC-1 $\alpha^{+/+}$ (n = 6), PGC-1 $\alpha^{-/-}$ (n = 7) and BicPGC-1 $\alpha^{-/-}$ (n = 7).

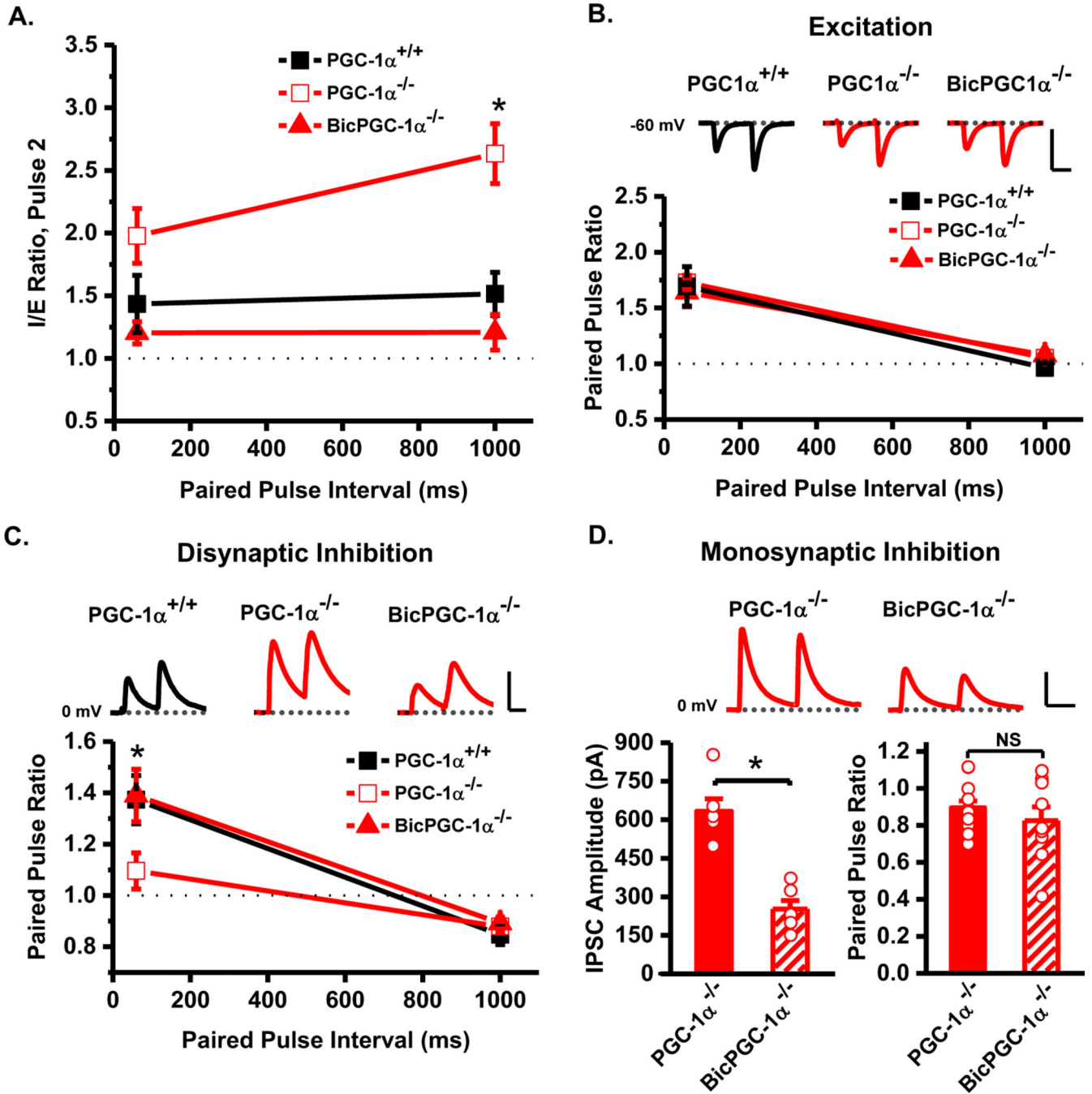


Figure 3. Bic rescues frequency dependent I/E ratio in PGC-1 $\alpha^{-/-}$ mice.

A: The I/E ratio on the second pulse at the 1000 ms interpulse interval is significantly enhanced in PGC-1 $\alpha^{-/-}$ slices compared to PGC-1 $\alpha^{+/+}$ slices, and this was rescued by Bic treatment. Surprisingly, Bic did not cause the second pulse of the I/E ratio at the 60 ms interval to be reduced below wild type levels (Two-way ANOVA, $F_{(2,50)} = 26.30$, $p < 0.000001$). * indicates significant difference from PGC-1 $\alpha^{+/+}$ and BicPGC-1 $\alpha^{-/-}$ slices. **B:** The paired-pulse ratio of the excitation is unchanged among the three groups (Two-way ANOVA, $F_{(2,50)} = 0.241$, $p = 0.786$). Insets, example traces of EPSCs from PGC-1 $\alpha^{+/+}$,

PGC-1 $\alpha^{-/-}$ and BicPGC-1 $\alpha^{-/-}$ slices at 60 ms inter-pulse interval. Scale bars, 30 ms, 200 pA. **C:** The paired pulse ratio of disynaptic inhibition shows facilitation in PGC-1 $\alpha^{+/+}$ slices and lower facilitation in PGC-1 $\alpha^{-/-}$ slices. Bic treatment enhanced the paired pulse facilitation back to PGC-1 $\alpha^{+/+}$ levels in PGC-1 $\alpha^{-/-}$ slices (Two way ANOVA, $F_{(2,50)} = 4.25$, $p = 0.019$). Insets, example traces of IPSCs from PGC-1 $\alpha^{+/+}$, PGC-1 $\alpha^{-/-}$ and BicPGC-1 $\alpha^{-/-}$ slices at 60 ms inter-pulse interval. Scale bars, 30 ms, 200 pA. For A-C: PGC-1 $\alpha^{+/+}$ ($n = 8$), PGC-1 $\alpha^{-/-}$ ($n = 13$) and BicPGC-1 $\alpha^{-/-}$ ($n = 7$); **D:** Monosynaptic IPSC amplitude significantly decreased after addition of 1 μ M Bic in PGC-1 $\alpha^{-/-}$ slices ($t_{(10)} = 6.45$, $p = 0.00007$). For monosynaptic IPSC: PGC-1 $\alpha^{-/-}$ slices ($n = 6$) and BicPGC-1 $\alpha^{-/-}$ slices ($n = 6$). However, 1 μ M Bic did not change the paired pulse ratio of monosynaptic IPSCs in slices from PGC-1 $\alpha^{-/-}$ mice, indicating no change in presynaptic release of GABA ($t_{(19)} = 0.89$, $p = 0.38$). Insets, example traces of IPSCs from PGC-1 $\alpha^{-/-}$ and BicPGC-1 $\alpha^{-/-}$ slices at 60 ms inter-pulse interval. Scale bars, 30 ms, 200 pA. For PPR monosynaptic IPSC: PGC-1 $\alpha^{-/-}$ slices ($n = 12$) and BicPGC-1 $\alpha^{-/-}$ slices ($n = 9$).

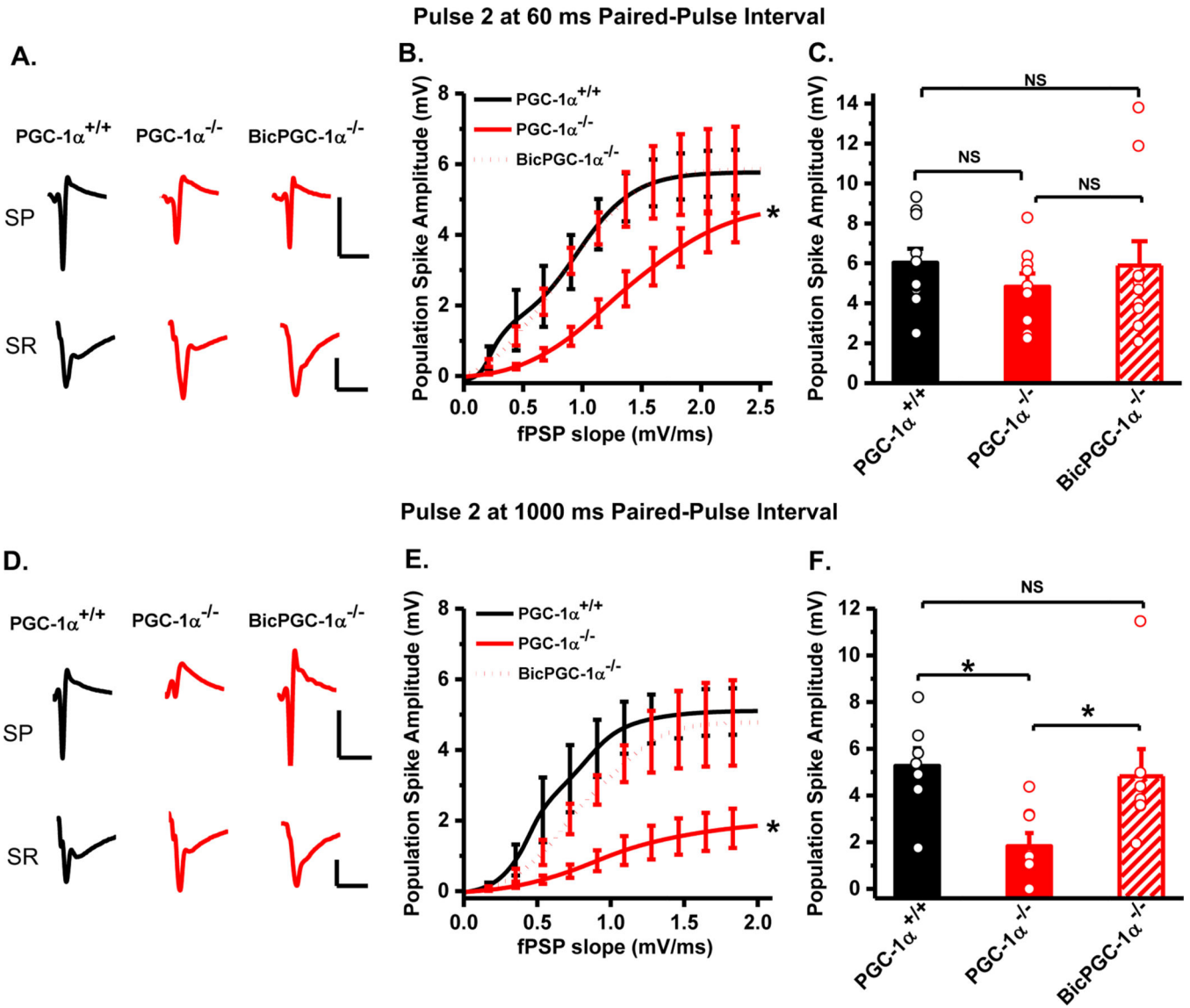


Figure 4. Bic rescues CA1 output at low and high frequencies as measured with E-S coupling on pulse 2 of paired-pulse stimulation.

A: Example traces of pulse 2 at 60 ms interpulse interval from field recordings in SP and SR from PGC-1 $\alpha^{+/+}$, PGC-1 $\alpha^{-/-}$ and BicPGC-1 $\alpha^{-/-}$ slices. Scale bars, 10 ms, 3 mV **B:** On the second pulse at 60 ms interval, the output from CA1 pyramidal cells in PGC-1 $\alpha^{-/-}$ slices was reduced compared to PGC-1 $\alpha^{+/+}$ slices (Two-way ANOVA, $F_{(2,724)} = 50.1$, $p < 0.000001$); PGC-1 $\alpha^{+/+}$ (n = 10), PGC-1 $\alpha^{-/-}$ (n = 9) and BicPGC-1 $\alpha^{-/-}$ (n = 10). The addition of 1 μ M bicuculline to PGC-1 $\alpha^{-/-}$ slices brought E-S coupling back to wild type levels. * indicates significant difference from PGC-1 $\alpha^{+/+}$ and BicPGC-1 $\alpha^{-/-}$ slices. **C:** The maximum population spike generated was plotted for the three groups at 60 ms interpulse interval showing no significant difference between the three groups (One-way ANOVA, $F_{(2,26)} = 0.50$, $p = 0.61$); PGC-1 $\alpha^{+/+}$ (n = 10), PGC-1 $\alpha^{-/-}$ (n = 9) and BicPGC-1 $\alpha^{-/-}$ (n = 10). **D:** Example traces of pulse 2 at 1000 ms interpulse interval from field recordings in SP and SR from PGC-1 $\alpha^{+/+}$, PGC-1 $\alpha^{-/-}$ and BicPGC-1 $\alpha^{-/-}$ slices. Scale bars, 10 ms, 3mV. **E:**

On pulse 2 at 1000 ms interval, the output from CA1 pyramidal cells for both PGC-1 $\alpha^{+/+}$ and BicPGC-1 $\alpha^{-/-}$ slices differ from PGC-1 $\alpha^{-/-}$ slices (Two-way ANOVA, $F_{(2,549)} = 115.5$, $p < 0.000001$); PGC-1 $\alpha^{+/+}$ (n = 7), PGC-1 $\alpha^{-/-}$ (n = 8) and BicPGC-1 $\alpha^{-/-}$ (n = 7), similar to pulse 1 (Figure 2B). * indicates significant difference from PGC-1 $\alpha^{+/+}$ and BicPGC-1 $\alpha^{-/-}$ slices. *F*: The maximum population spike amplitude on pulse 2 at 1000 ms interpulse interval is reduced in PGC-1 $\alpha^{-/-}$ slices and restored by Bic. (One-way ANOVA, $F_{(2,19)} = 5.16$, $p = 0.016$); PGC-1 $\alpha^{+/+}$ (n = 7), PGC-1 $\alpha^{-/-}$ (n = 8) and BicPGC-1 $\alpha^{-/-}$ (n = 7).

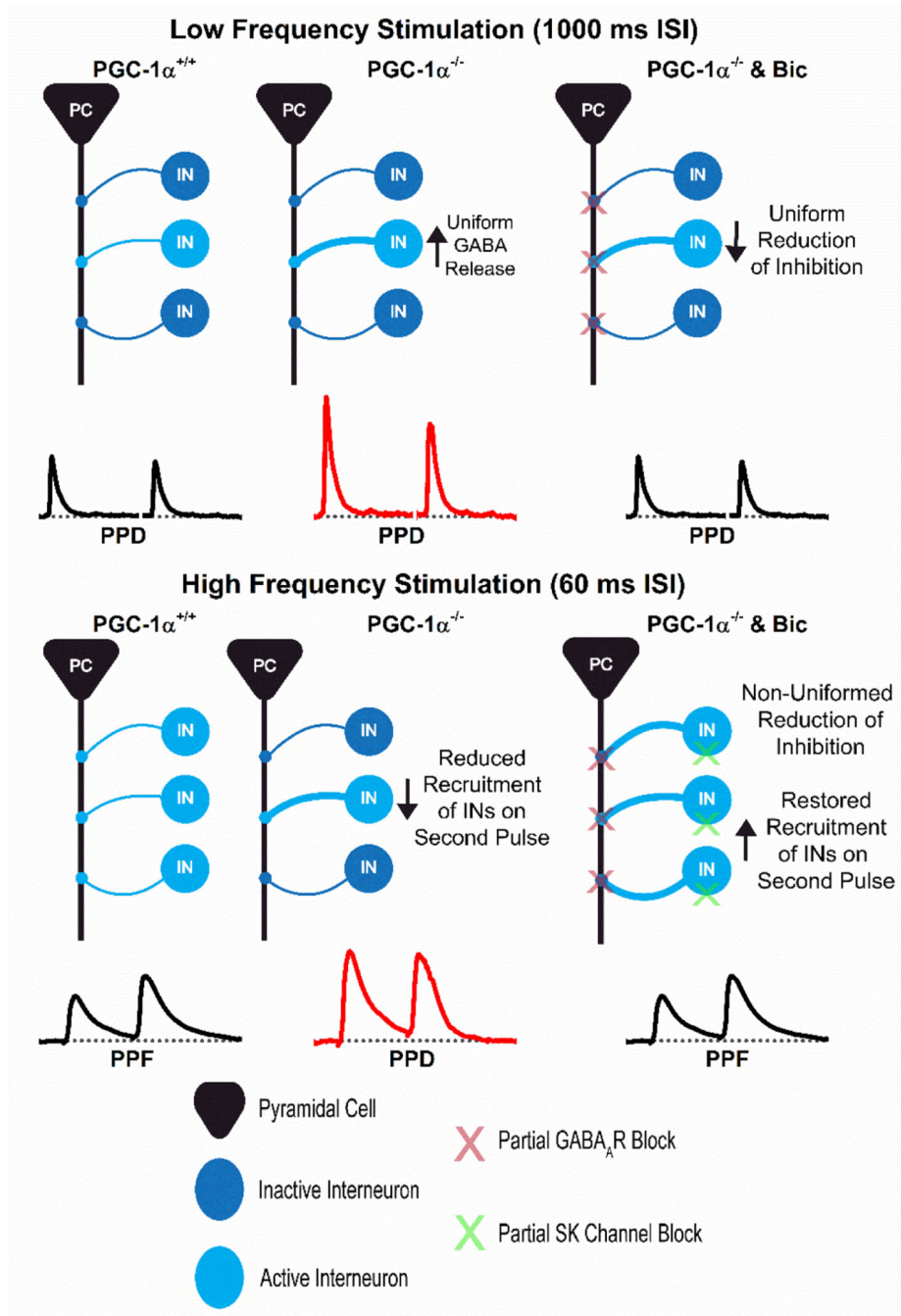


Figure 5. Bic rescues disynaptic inhibition in a frequency-dependent manner.

A schematic depicting the underlying circuit changes that occur in the three conditions (PGC-1 $\alpha^{+/+}$, PGC-1 $\alpha^{-/-}$, and PGC-1 $\alpha^{-/-}$ plus 1 μ M bicuculline) and the expected disynaptic IPSC response. The top half depicts what is happening at low frequency stimulation. This shows that bicuculline reduces inhibition in a uniform manner (to the same extent on pulse 2 as pulse 1), consistent with effects of blocking GABA_A receptors on pyramidal cells, and therefore does not alter short-term plasticity of disynaptic inhibition. The bottom half depicts what is happening at high frequency stimulation (e.g. second pulse

at 60 ms). Bicuculline reduces inhibition in a non-uniform manner (greater reduction on pulse 1 than pulse 2). This shows that bicuculline is most likely also increasing recruitment of interneurons on the second pulse, potentially through blockade of SK channels or reduced inhibition onto GABAergic interneurons, which allows the short-term plasticity to be restored to PPF.

Author Manuscript

Author Manuscript

Author Manuscript

Author Manuscript